J|A|C|S
ARTICLES
Published on Web 02/10/2006

Theoretical Investigation of Enolborane Addition to α-Heteroatom-Substituted Aldehydes. Relevance of the Cornforth and Polar Felkin−Anh Models for Asymmetric Induction

Victor J. Cee,[†] Christopher J. Cramer,*[,‡] and David A. Evans*[,†]

Contribution from the Department of Chemistry and Chemical Biology, Harvard University, Cambridge, Massachusetts 02138, and Department of Chemistry and Supercomputing Institute, University of Minnesota, Minneapolis, Minnesota 55455

Received August 25, 2005; E-mail: cramer@chem.umn.edu; evans@chemistry.harvard.edu

Abstract: The addition of enolborane nucleophiles to chiral α-heteroatom-substituted aldehydes ($CH_3CH(X)CHO$, X = F, Cl, OMe, SMe, NMe_2, and PMe_2) was investigated using density functional theory by means of B3LYP/6-31G(d) calculations, with particular emphasis on determining the relevance of the polar Felkin−Anh and Cornforth models for asymmetric induction in these reactions. The relative energy of the polar Felkin−Anh and Cornforth transition-state structures is found to depend on the nature of the α-heteroatom substituent, with electronegative substituents (F, OMe, Cl) favoring Cornforth structures, while less electronegative substituents (PMe_2, SMe, NMe_2) favor polar Felkin−Anh structures. These transition-state preferences are correlated with the relative energy of the corresponding rotamer of the uncomplexed reactant aldehyde, indicating that the transition states are particularly sensitive to the conformation of the aldehyde. The proposed Nu → σ^*_{C-X} interaction that forms the basis of the polar Felkin−Anh model appears to be insignificant in reactions with enolborane nucleophiles. The calculated transition-state structures for the addition of *E*- and *Z*-enolborane nucleophiles to 2-methoxypropanal predict a diastereofacial selectivity that is in good agreement with the experimentally determined values.

Introduction

Different interpretations of the relative importance of steric, electronic, and torsional effects in nucleophilic addition reactions of α-substituted carbonyl compounds have led to an array of transition-state models.[1] The characteristic stereoinduction resulting from nucleophilic addition to carbonyl compounds bearing an adjacent heteroatom substituent (eq 1) is explained by both the Cornforth[2] and polar Felkin−Anh[3] (PFA) models. These models are based on different conformers deriving from rotation about the aldehyde C_1-C_2 bond. Ab initio studies of metal hydride and cyanide anion addition to chiral α-heteroatom-substituted aldehydes have generally supported the PFA model,[4,5] and this is likely responsible for its widespread popularity. A recent experimental study[6] of enolborane addition to α-alkoxy aldehydes was found to support the Cornforth model, rather than the PFA model.[7] This finding is inconsistent with the prevailing wisdom regarding transition-state models for asymmetric induction, and the following theoretical investigation was initiated to better understand the factors controlling asymmetric induction in enolborane additions to α-heteroatom-substituted aldehydes.[8]

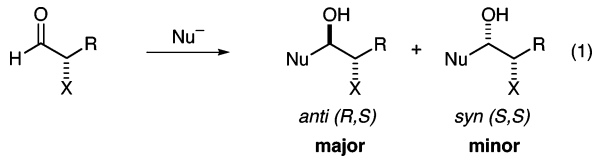

The addition of a nucleophile to an aldehyde bearing an adjacent α-heteroatom substituent under conditions in which

[†] Harvard University.
[‡] University of Minnesota.

(1) Mengel, A.; Reiser, O. *Chem. Rev.* **1999**, *99*, 1191−1223.
(2) Cornforth, J. W.; Cornforth, R. H.; Mathew, K. K. *J. Chem. Soc.* **1959**, 112−127. The Cornforth model discussed here is modified from its original form to incorporate contemporary concepts of a staggered arrangement about the forming C−Nu bond (ref 10) and a >90° angle of attack for the incoming nucleophile (ref 11).
(3) (a) Chérest, M.; Felkin, H.; Prudent, N. *Tetrahedron Lett.* **1968**, *18*, 2199−2204. (b) Chérest, M.; Felkin, H. *Tetrahedron Lett.* **1968**, *9*, 2005−2208. (c) Anh, N. T.; Eisenstein, O. *Nouv. J. Chim.* **1977**, *1*, 61−70. (d) Anh, N. T. *Top. Curr. Chem.* **1980**, *88*, 145−162. Carbonyl addition reactions in which the α-stereocenter of the electrophile is composed of substituents that differ by steric, rather than electronic, properties are also described by a Felkin−Anh model. In this case, the largest substituent occupies a position antiperiplanar to the incoming nucleophile. For a recent discussion of the utility of this model, see: (e) Smith, R. J.; Trzoss, M.; Bühl, M.; Bienz, S. *Eur. J. Org. Chem.* **2002**, 2770−2775.
(4) (a) Wu, Y.-D.; Houk, K. N. *J. Am. Chem. Soc.* **1987**, *109*, 908−910. (b) Wong, S. S.; Paddon-Row, M. N. *J. Chem. Soc., Chem. Commun.* **1990**, 456−458. (c) Wu, Y.-D.; Tucker, J. A.; Houk, K. N. *J. Am. Chem. Soc.* **1991**, *113*, 5018−5027. (d) Wong, S. S.; Paddon-Row, M. N. *J. Chem. Soc., Chem. Commun.* **1991**, 327−330. (e) Wong, S. S.; Paddon-Row, M. N. *Aust. J. Chem.* **1991**, *44*, 765−770. (f) Frenking, G.; Köhler, K. F.; Reetz, M. T. *Tetrahedron* **1991**, *47*, 9005−9018. (g) Frenking, G.; Köhler, K. F.; Reetz, M. T. *Tetrahedron* **1993**, *49*, 3983−3994. (h) Anh, N. T.; Maurel, F.; Lefour, J.-M. *New. J. Chem.* **1995**, *19*, 353−364.
(5) The following theoretical studies have supported transition-state features consistent with the Cornforth model. Addition of cyanide anion to fluoroacetaldehyde in solution: (a) Cieplak, A. S.; Wiberg, K. B. *J. Am. Chem. Soc.* **1992**, *114*, 9226−9227. Addition of cyanide anion to chlorofluoroacetaldehyde in the gas phase: (b) Frenking, G.; Köhler, K. F.; Reetz, M. T. *Tetrahedron* **1994**, *50*, 11197−11204.
(6) Evans, D. A.; Siska, S. J.; Cee, V. J. *Angew. Chem., Int. Ed.* **2003**, *42*, 1761−1765.

10.1021/ja0555670 CCC: $33.50

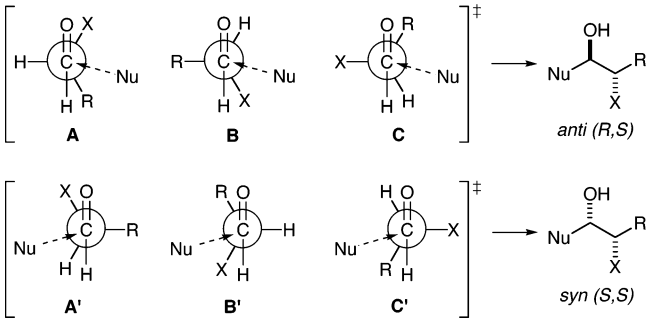

Figure 1. Staggered transition-state representations for nucleophilic addition.

chelate organization[9] is precluded generally proceeds with selectivity for the anti product diastereomer (eq 1). The origin of the stereoselectivity in these reactions has been the topic of study for five decades. Arguably one of the most important contributions to the evolution of modern carbonyl addition models is Felkin's conclusion in 1968 that staggered rather than eclipsed transition states best explain the wealth of experimental data.[3a,b] This postulate has subsequently been confirmed by the seminal transition-state modeling studies of Houk, Paddon-Row, and Rondan.[10] For additions to an α-heteroatom-substituted aldehyde, six staggered transition-state arrangements for addition to either π-face of the carbonyl can be identified (Figure 1).[11] These transition states are grouped with respect to the reacting carbonyl diastereoface (**A**−**C** vs **A′**−**C′**) and the relationship between the nucleophile and heteroatom substituent X. The following transition-state models are based on the simplifying assumption that two transition-state rotamers of opposite stereochemical outcomes are significantly stabilized and therefore govern the observed product ratio.

Polar Felkin−Anh Model. The PFA model is based on the Felkin premise[3a,b] that staggered transition states are preferred and Anh and Eisenstein's view that the principal transition-state stabilizing interaction is hyperconjugative delocalization of the forming bond (HOMO) with the best vicinal acceptor, the C−X bond (LUMO).[3c] The hyperconjugative interaction will be maximized when the forming bond and the C−X bond are antiperiplanar, as in transition states **C** and **C′** (Figure 2). These transition states are further distinguished by steric interactions between the nucleophile and α-substituents. In the transition

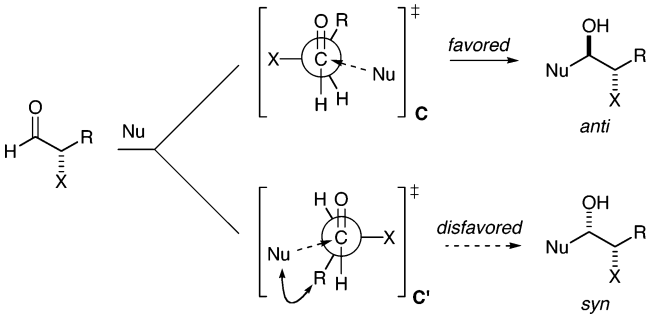

Figure 2. The polar Felkin−Anh model.

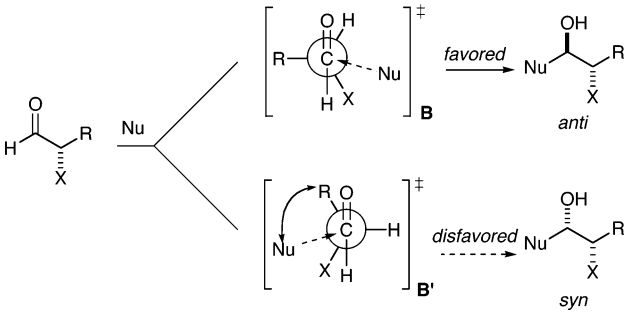

Figure 3. The Cornforth model.

state leading to the anti product diastereomer (**C**), the nucleophile approaches in close proximity to a hydrogen atom, while the transition state leading to the syn product diastereomer (**C′**) is destabilized by the proximity of the nucleophile and the alkyl substituent.

Cornforth Model. The Cornforth model, presented in 1959, was provided as a rationalization for the stereoselective additions of Grignard reagents to α-chloro aldehydes and ketones.[2] This model embraces the assumption that electrostatic (dipole) effects are instrumental in dictating an antiparallel dihedral angle relationship between the carbonyl and the α-Cl substituent. From this conformation, nucleophilic addition could then be predicted on the basis of a steric argument taking into consideration the relative "sizes" of the remaining α-substituents. In the modern rendition of the Cornforth model, Felkin's staggered transition states[3a,b] may now be incorporated (Figure 3). The two relevant transition states **B** and **B′** having the electronegative substituent and carbonyl in a dipole-minimized orientation can be further distinguished by steric interactions. In the transition state leading to the anti product diastereomer (**B**), the nucleophile approaches between the heteroatom substituent and a hydrogen atom. The transition state leading to the syn product diastereomer (**B′**) is destabilized by the proximity of the nucleophile to the alkyl substituent.

Theoretical Design. The primary concern of this study is to establish the relevance of the PFA and Cornforth models in the addition of enolborane nucleophiles to α-heteroatom-substituted aldehydes. The aldol reaction between acetaldehyde enolborane **7** and propanals substituted in the α-position with first- and second-row monovalent (**1** X = F, **2** X = Cl), divalent (**3** X = OMe, **4** X = SMe), and trivalent (**5** X = NMe_2, **6** X = PMe_2) heteroatoms was chosen as a computationally reasonable system (Scheme 1). The effect of enolate substitution was examined in the reaction of propanal enolborane **8** and aldehyde **3**. Only chairlike transition-state structures with an equatorially disposed aldehyde substituent were considered. While the reactions of

(7) Similar conclusions have been drawn for the mechanistically related crotylboronate nucleophiles: (a) Hoffmann, R. W. *Chem. Scr.* **1985**, *25* (Special Issue), 53−60. (b) Roush, W. R.; Adam, M. A.; Walts, A. E.; Harris, D. J. *J. Am. Chem. Soc.* **1986**, *108*, 3422−3434. (c) Hoffmann, R. W.; Metternich, R.; Lanz, J. W. *Liebigs Ann. Chem.* **1987**, 881−887. (d) Brinkmann, H.; Hoffmann, R. W. *Chem. Ber.* **1990**, 2395−2401.

(8) Theoretical studies of related nucleophilic addition processes have been previously reported. A study of the allylboration of 2-methoxypropanal has supported the Cornforth model: (a) Gung, B. W.; Xue, X. *Tetrahedron: Asymmetry* **2001**, *12*, 2955−2959. A limited study of lithium enolate addition to 2-methoxypropanal has supported the polar Felkin−Anh model: (b) Arrastia, I.; Lecea, B.; Cossío, F. P. *Tetrahedron Lett.* **1995**, *36*, 245−248.

(9) For a review of chelation-controlled nucleophilic additions, see: (a) Reetz, M. T. *Angew. Chem., Int. Ed. Engl.* **1984**, *23*, 556−569. (b) Reetz, M. T. *Acc. Chem. Res.* **1993**, *26*, 462−468. For experimental evidence of chelates as reactive intermediates, see: (c) Chen, X.; Hortelano, E. R.; Eliel, E. L.; Frye, S. V. *J. Am. Chem. Soc.* **1992**, *114*, 1778−1784.

(10) Paddon-Row, M. N.; Rondan, N. G.; Houk, K. N. *J. Am. Chem. Soc.* **1982**, *104*, 7162−7166. (b) Houk, K. N.; Paddon-Row, M. N.; Rondan, N. G.; Wu, Y.-D.; Brown, F. K.; Spellmeyer, D. C.; Metz, J. T.; Li, Y.; Longarich, R. J. *Science* **1986**, *231*, 1108−1117.

(11) For historical reasons, the transition states are depicted as Newman projections of reactant aldehyde conformers with the nucleophile approaching at the Bürgi−Dunitz trajectory. (a) Bürgi, H. B.; Dunitz, J. D.; Shefter, E. *J. Am. Chem. Soc.* **1973**, *95*, 5065−5067. (b) Bürgi, H. B.; Dunitz, J. D.; Lehn, J. M.; Wipff, G. *Tetrahedron* **1974**, *30*, 1563−1572.

Scheme 1. Enolborane Addition to Heteroatom-Substituted Propanals

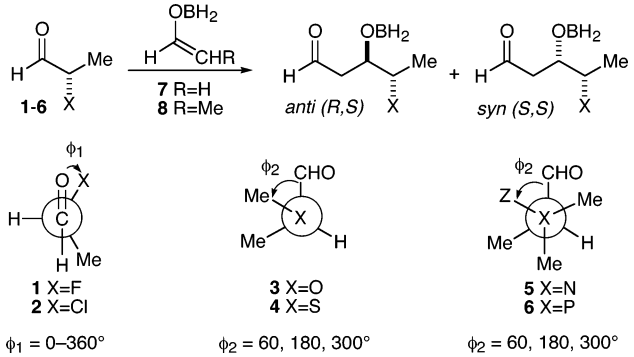

acetaldehyde enolborane are certainly not limited to this arrangement, the chair geometry is believed to be predominant in reactions of substituted enolboranes, for which experimental data are available.

The halopropanals **1** and **2** (Scheme 1) represent the simplest heteroatom-substituted aldehydes and consequently were studied in the most detail. Rotamers of these aldehydes are conveniently described by the OCCX dihedral angle ϕ_1. Transition-state structures were optimized for enolborane addition to both aldehyde π-faces with ϕ_1 ranging from 0 to 360° in increments of 30°.[12] Aldehydes **3**−**6** which contain divalent and trivalent substituents are significantly more complex due to additional rotational isomerism about the C−X bond. The rotamers of aldehydes **3** and **4** are described by both ϕ_1 and the CCXC dihedral angle ϕ_2. In the case of aldehydes **5** and **6**, ϕ_2 is defined as the CCXZ dihedral angle, in which Z is an imaginary atom in the plane that bisects the Me−X−Me angle. Due to the increased complexity of aldehydes **3**−**6**, transition-state structures were optimized at all values of ϕ_2 which define staggered rotamers at values of ϕ_1 corresponding to Cornforth or PFA rotamers.

Computational Methods

All calculations were carried out using methods and basis sets implemented in the Gaussian package of programs (G98.A11).[13] The hybrid Hartree−Fock density functional B3LYP method[14] with the 6-31G(d) basis set[15] was used; in some cases the 6-311+G(3df,2p) basis set[15] was employed for comparison. Second-order perturbation theory (MP2) with the 6-31G(d) or 6-311+G(3df,2p) basis sets was also occasionally employed for comparison.[16] All reactant and transition-state structures obtained by unconstrained optimization, with the exception of MP2/6-311+G(3df,2p) structures, were characterized by vibrational frequency analysis. The zero-point energies determined for these structures are not included in the reported energies in order to facilitate comparison with structures optimized at fixed angles. The NBO 4.0 program[17] was used as implemented in the Gaussian 98 package, and the reported NBO delocalization energies (E2) are those given by second-order perturbation theory.

Scheme 2. Theoretical Methods for the Study of Enolborane Addition Reactions

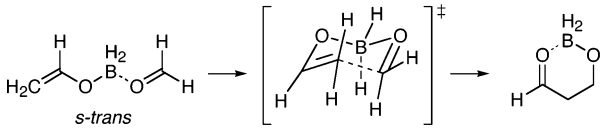

Results and Discussion

Theoretical Validation. While the combination of B3LYP and the 6-31G(d) basis set has been shown to be generally robust for a large number of organic reactions, it was of interest to compare it to second-order perturbation theory (MP2) using the same basis set for an elementary enolborane addition reaction (Scheme 2).[18] At the MP2 level, the aldol reaction between acetaldehyde enolborane and formaldehyde is predicted to be exoergic by 25.3 kcal/mol with an activation energy of 4.6 kcal/mol. At the B3LYP level, these values are 25.4 and 3.0 kcal/mol, respectively. The geometries of the transition-state structures predicted by the two methods are quite similar. At the B3LYP level, the nucleophile approaches the carbonyl at a 102.7° angle of attack[19] with a 2.34 Å length for the forming C−C bond. At the MP2 level, these values are 103.0° and 2.31 Å, respectively. The only significant difference between the two methods is a 1.6 kcal/mol discrepancy in the magnitude of the barrier height for enolborane addition. This difference is of little consequence to the present investigation, which is concerned with the relative energies of activation for addition to different aldehyde rotamers. Additional comparisons of B3LYP and MP2 for enolborane addition to aldehydes **1** and **2** indicate excellent agreement in this regard (vide infra).

The effectiveness of B3LYP/6-31G(d) in modeling the conformational properties of α-heteroatom-substituted aldehydes was determined for fluoroacetaldehyde and chloroacetaldehyde. Although only a small amount of experimental data is available to validate the theoretical results, the effect of method and basis set on the calculated rotational energy profile and predicted conformational equilibrium can be established. The rotational profiles presented in Figures 4 and 5 were generated by optimization of the aldehyde geometry at a fixed value of ϕ_1 (0−180° in 15° increments).

There is generally good agreement between the different levels of theory for the rotational profile of fluoroacetaldehyde (Figure 4), with the exception of the MP2/6-31G(d) results for small values of ϕ_1. The fully optimized conformational minima and the transition-state structure for their interconversion were obtained by optimization with no constraint on the dihedral angle (Table 1). The conformation with the C═O and C−F bonds eclipsed ($\phi_1 = 0°$) is calculated at the B3LYP/6-31G(d) level

(12) To be precise, such structures have the status of true transition-state structures within the 3*N*-7-dimensional spaces defined by removing the coordinate ϕ_1 from the 3*N*-6 internal coordinates (where *N* is the number of atoms) characterizing each system.
(13) Frisch, M. J.; et al. Gaussian 98 (revision A.11); Gaussian Inc.: Pittsburgh, PA, 2001.
(14) (a) Becke, A. D. *Phys. Rev. A* **1988**, *38*, 3098−3100. (b) Lee, C.; Yang, W.; Parr, R. G. *Phys. Rev. B* **1988**, *37*, 785−789. (c) Becke, A. D. *J. Chem. Phys.* **1993**, *98*, 5648−5652. (d) Stephens, P. J.; Devlin, F. J.; Chabalowski, C. F.; Frisch, M. J. *J. Phys. Chem.* **1994**, *98*, 11623−11627.
(15) Hehre, W. J.; Radom, L.; Schleyer, P. v. R.; Pople, J. A. *Ab Initio Molecular Orbital Theory*; Wiley: New York, 1986.
(16) Cramer, C. J. *Essentials of Computational Chemistry: Theories and Models*; Wiley: Chichester, 2002.
(17) Glendening, E. D.; Badenhoop, J. K.; Reed, A. E.; Carpenter, J. E.; Weinhold, F. F. *NBO 4.0*; Theoretical Chemistry Institute, University of Wisconsin: Madison, WI, 1996.
(18) Houk and co-workers have previously reported an activation energy of 8.2 kcal/mol and exoergicity of 25.6 kcal/mol for this process at the HF/6-31G(d)//HF/3-21G level: Li, Y.; Paddon-Row, M. N.; Houk, K. N. *J. Org. Chem.* **1990**, *55*, 481−493.
(19) The transition-state structures reported here are characterized by a narrow range of attack angles. For acetaldehyde enolborane, the angle ranges from 102 to 104°; for propanal enolborane, the range is 104−106°.

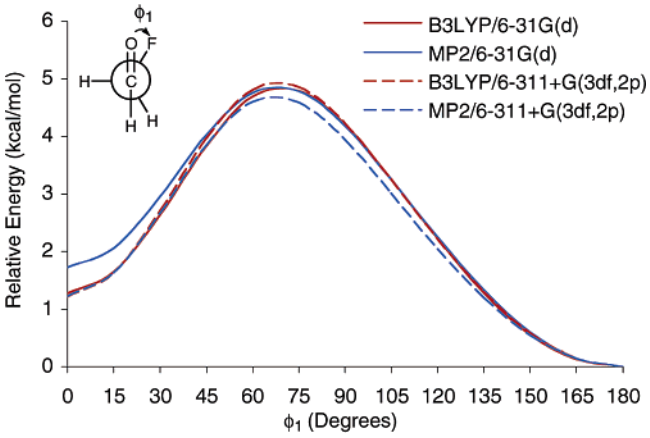

Figure 4. Calculated rotational energy profile of fluoroacetaldehyde.

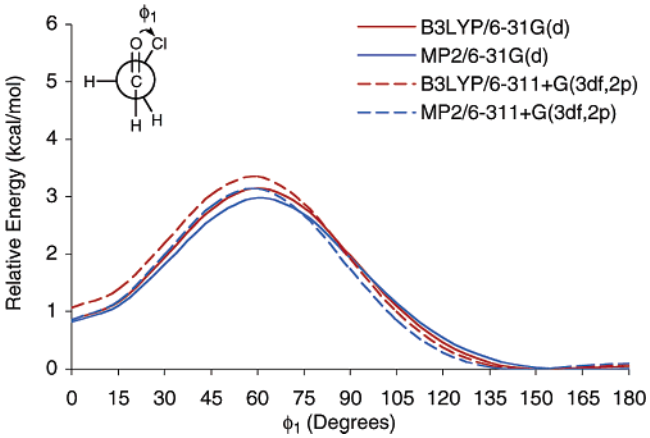

Figure 5. Calculated rotational energy profile of chloroacetaldehyde.

Table 1. Relative Energies for Fully Optimized Fluoroacetaldehyde Structures[a]

method	ΔE (anti-eclipsed)	$\Delta E^{\ddagger}$ (TS-anti)
B3LYP/6-31G(d)	1.27	4.85
MP2/6-31G(d)	1.71	4.87
B3LYP/6-311+G(3df,2p)	1.21	4.93
MP2/6-311+G(3df,2p)	1.23	4.69

[a] Relative energy is given in kcal/mol.

to be 1.27 kcal/mol higher in energy than the conformer in which these groups are antiperiplanar ($\phi_1 = 180°$), with a 4.85 kcal/mol barrier for the anti to eclipsed rotation. The B3LYP/6-31G(d) level is sufficient for the study of fluorine-substituted aldehydes, as evidenced by its consistency with calculations employing larger basis sets.

The profile for chloroacetaldehyde (Figure 5) exhibits slightly more variation, but B3LYP/6-31G(d) appears to be a good compromise between the different methods. Stable minima include the eclipsed conformation at $\phi_1 = 0$ and a skew conformation at a dihedral angle of approximately 150°. The antiperiplanar arrangement at $\phi_1 = 180°$ is now slightly destabilized, in good agreement with experimental[20] and theoretical[21] data. The energy difference between the conformational minima is calculated at the B3LYP/6-31G(d) level to be 0.86 kcal/mol favoring the skew arrangement, with a 3.14 kcal/mol barrier for the skew to eclipsed rotation (Table 2). An IR study of chloroacetaldehyde reports the skew-eclipsed energy difference to be 0.76 ± 0.05 kcal/mol, with a 1.43 ± 0.01 kcal/mol barrier for the skew to eclipsed rotation.[22] While the agreement between theory and experiment for the skew-eclipsed energy difference is satisfying, the disagreement in the barrier to rotation by a factor of 2 is a cause for concern,[23] and this clearly requires further theoretical and experimental investigation. The theoretically derived conformational energy parameters are at least consistent with respect to different methods and basis sets, indicating that the B3LYP/6-31G(d) level does not suffer from any deficiencies relative to the other levels studied.

Table 2. Relative Energies for Fully Optimized Chloroacetaldehyde Structures[a]

method	ΔE (skew-eclipsed)	$\Delta E^{\ddagger}$ (TS-skew)
B3LYP/6-31G(d)	0.86	3.14
MP2/6-31G(d)	0.83	2.98
B3LYP/6-311+G(3df,2p)	1.06	3.35
MP2/6-311+G(3df,2p)	0.87	3.15
IR (experimental)	0.76 ± 0.05	1.43 ± 0.01

[a] Relative energy is given in kcal/mol.

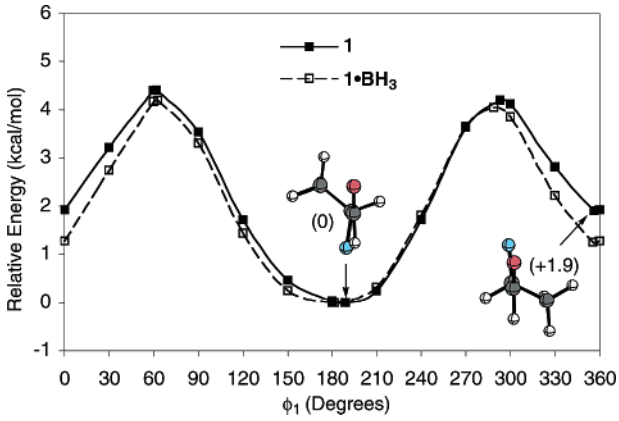

Figure 6. Rotational energy profile of **1** and **1·BH$_3$** (red = O, blue = F).

Rotational Energy Profile of 1. 2-Fluoropropanal (**1**) is characterized by a 2-fold rotational energy profile (Figure 6). Stable conformers occur at $\phi_1 = 189$ and 356°, in which the C−F bond is nearly antiparallel to or eclipsing the C═O bond, respectively. The presence of a stable antiparallel arrangement is somewhat unusual for a substituted aldehyde, since this necessarily results in a conformation in which no substituent eclipses the C═O bond.[24] This appears to be unique to aldehydes containing highly electronegative substituents, such as fluorine and oxygen.[25] The antiparallel conformation ($\phi_1 = 189°$) is calculated to be 1.9 kcal/mol more stable than the eclipsed

(20) Microwave spectroscopy: (a) Ford, R. G. *J. Chem. Phys.* **1976**, *65*, 354−362. (b) Malloy, T. B., Jr.; Carreira, L. A. *J. Chem. Phys.* **1977**, *66*, 4246−4247. Gas-phase electron diffraction: (c) Dyngeseth, S.; Schei, H.; Hagen, K. *J. Mol. Struct.* **1983**, *102*, 45−54. For an NMR study of chloroacetaldehyde in solution, see: (d) Karabatsos, G. J.; Fenoglio, D. J. *J. Am. Chem. Soc.* **1969**, *91*, 1124−1129.

(21) (a) Durig, J. R.; Phan, H. V.; Little, T. S.; Van Der Veken, B. J. *J. Mol. Struct. (THEOCHEM)* **1989**, *202*, 143−157. (b) Frenking, G.; Köhler, K. F.; Reetz, M. T. *Tetrahedron* **1991**, *47*, 8991−9004. (c) Pontes, R. M.; Fiorin, B. C.; Basso, E. A. *Chem. Phys. Lett.* **2004**, *395*, 205−209. For a semiempirical study of α-heteroatom-substituted aldehydes in solution, see: (d) Varnali, T.; Aviyente, V.; Terryn, B.; Ruiz-López, M. F. *J. Mol. Struct. (THEOCHEM)* **1993**, *280*, 169−179.

(22) Durig, J. R.; Phan, H. V.; Little, T. S.; Tolley, C. L. *Struct. Chem.* **1990**, *1*, 459−472.

(23) The 6-31G(d) basis set has been shown to be adequate for reproducing the experimentally determined barrier to rotation for acetaldehyde and propanal: Wiberg, K. B.; Martin, E. *J. Am. Chem. Soc.* **1985**, *107*, 5035−5041.

(24) In contrast, the two stable conformers of propanal have been shown to have either the C−C or C−H bond eclipsing the carbonyl. See: Butcher, S. S.; Wilson, E. B. *J. Chem. Phys.* **1964**, *40*, 1671−1678.

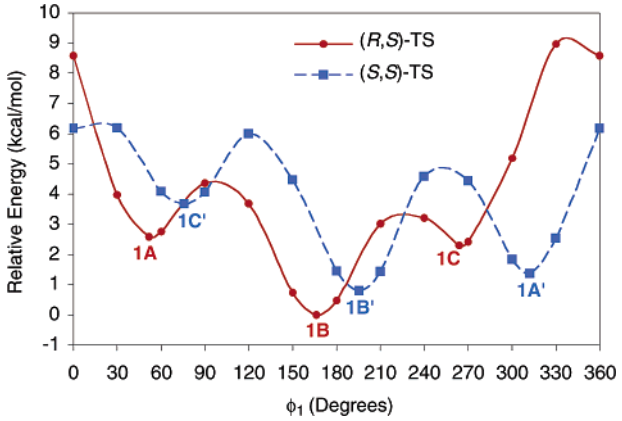

Figure 7. Relative TS energy for enolborane addition to **1** as a function of dihedral angle ϕ_1.

conformation ($\phi_1 = 356°$). Complexation of **1** with BH_3 does not change the shape of the profile significantly,[26] but does reduce the energy difference between the two stable conformations by a small amount to 1.3 kcal/mol.

Transition-State Profile for Addition to 1. The rotational energy profile for enolborane addition to aldehyde **1** is presented in Figure 7. The curves represent relative energies for transition-state structures optimized at fixed values of the dihedral angle ϕ_1 in increments of 30°. The minima were obtained by full optimizations without constraints. Addition to either aldehyde π-face is characterized by three minima and three maxima. The minima correspond to structures containing a staggered arrangement about the forming C−C bond, while the maxima correspond to eclipsed arrangements.

The B3LYP/6-31G(d) transition-state structures obtained by full optimization without constraints are presented along with their relative energies in Figure 8.[27] The lowest energy structures for the formation of the anti (*R*,*S*) and syn (*S*,*S*) products occur at $\phi_1 = 166°$ (**1B**) and $\phi_1 = 196°$ (**1B′**), respectively. These structures both contain nearly antiparallel arrangements of C═O and C−F bonds, corresponding to the Cornforth transition-state model (Figure 3). The destabilization of structure **1B′** (+0.8 kcal/mol) relative to **1B** is likely due to the additional gauche interaction in **1B′** between the α-methyl substituent and the forming C−C bond. Structures **1C** and **1C′** (at $\phi_1 = 264$ and 76°, respectively) are characterized by an antiperiplanar relationship between the forming C−C bond and the C−F bond, corresponding to the polar Felkin−Anh model. In this case, these structures are significantly destabilized (**1C**, +2.4; **1C′**, +3.7 kcal/mol) relative to **1B**. Therefore, the Cornforth rotamers **1B** and **1B′** are the most significant transition-state structures for enolborane addition to 2-fluoropropanal, with stereoinduction favoring the anti product diastereomer due to fewer gauche relationships in **1B**.

The extent of C−C bond formation in the transition state can be assessed by determining the distance between the reacting carbon atoms of the aldehyde and enolborane (Figure 9). Although substantial variation in this distance is observed, the minimum energy transition-state structures span a narrow range of C−C distances (2.22−2.27 Å), indicating a relatively early transition state. The involvement of the C−F bond in the Nu → σ^*_{C-F} hyperconjugative interaction believed to stabilize PFA transition states **C** and **C′** can be assessed by comparing the C−F bond lengths in the transition-state structures and reactant aldehyde structures (Figure 10).[28] Indeed, **1C** and **1C′** are characterized by relatively long C−F bonds (1.404 Å for **1C** and **1C′**), which suggests that the C−F bond is involved in a hyperconjugative interaction. However, this bond lengthening is not significantly greater than that already present in the reactant aldehyde **1** (C−F range: 1.381−1.404 Å), and it may be concluded that a Nu → σ^*_{C-F} hyperconjugative interaction is absent in this system.

Rotational Energy Profile of 2. 2-Chloropropanal (**2**) is characterized by a 3-fold rotational energy profile (Figure 11), with a wide, flat region between $\phi_1 = 120$ and 240°. The profile is consistent with that calculated at the MP2/6-31G(d)//HF/6-31G(d) level by Frenking and co-workers.[21b] In contrast to 2-fluoropropanal, a small maximum exists in the vicinity of 180°, with two minima occurring on either side at $\phi_1 = 136$ and 225°.[29] The other minimum at $\phi_1 = 357°$ contains a parallel arrangement of C═O and C−Cl bonds and is significantly higher in energy. Complexation of **2** with BH_3 results in only modest changes in the shape of the rotational profile.

Transition-State Profile for Addition to 2. The rotational energy profile for enolborane addition to aldehyde **2** is presented in Figure 12. The shape of the profile resembles that of 2-fluoropropanal, although the relative positions of some minima are different. The transition-state structures obtained by full optimization without constraints are presented along with their relative energies in Figure 13.[30] The lowest energy structures for the formation of the anti (*R*,*S*) and syn (*S*,*S*) product diastereomers occur at $\phi_1 = 175°$ (**2B**) and $\phi_1 = 186°$ (**2B′**), respectively. These structures both contain nearly antiparallel arrangements of C═O and C−Cl bonds, corresponding to the Cornforth transition-state model (Figure 3). Structures **2C** and **2C′** (at $\phi_1 = 267$ and 76°, respectively) are characterized by an antiperiplanar relationship between the forming C−C bond and the C−Cl bond, corresponding to the polar Felkin−Anh model (Figure 2). In contrast to 2-fluoropropanal, these structures are now much closer in energy to **2B** (**2C**, +0.2; **2C′**, +1.7 kcal/mol). Therefore, the Cornforth rotamers **2B** and **2B′** as well as the PFA rotamer **2C** are the most significant transition-state structures for enolborane addition to 2-chloropropanal.

The extent of C−C bond formation in the transition state for enolborane addition to **2** can be assessed by determining the distance between the reacting carbon atoms of the aldehyde and

(25) For theoretical investigations of 2-methoxypropanal conformers, see: (a) Frenking, G.; Köhler, K. F.; Reetz, M. T. *Tetrahedron* **1993**, *49*, 3971−3982. (b) Lecea, B.; Arrieta, A.; Cossío, F. P. *J. Org. Chem.* **1997**, *62*, 6485−6492.
(26) Lepage, T. J.; Wiberg, K. B. *J. Am. Chem. Soc.* **1988**, *110*, 6642−6650.
(27) At the MP2/6-31G(d) level, the relative energies (in kcal/mol) of transition-state structures for enolborane addition to **1** are: **1A** (+3.0), **1B** (0), **1C** (+2.2), **1A′** (+1.5), **1B′** (+0.8), **1C′** (+4.0).
(28) This analysis is not able to distinguish between involvement of the C−X bond as a donor or acceptor in a hyperconjugative interaction, since in both cases an increase in the C−X bond length would be expected. The generalized anomeric effect is characterized by C−X bond lengthening associated with $n_Y \rightarrow \sigma^*_{C-X}$ delocalization: (a) Schleyer, P. v. R.; Kos, A. J. *Tetrahedron* **1983**, *39*, 1141−1150. (b) Juaristi, E.; Cuevas, G. *Tetrahedron* **1992**, *48*, 5019−5087. The dihedral angle-dependent C−Cl bond lengthening in α-chloro ketones is believed to be due to $\sigma_{C-Cl} \rightarrow \pi^*_{C=O}$ delocalization: (c) Laube, T.; Ha, T.-K. *J. Am. Chem. Soc.* **1988**, *110*, 5511−5517.
(29) The calculated conformational minima are in good qualitative agreement with experimental data obtained from gas-phase electron diffraction: Aarset, K.; Hagen, K.; Frenking, G.; Wehrsig, A. *J. Phys. Chem.* **1993**, *97*, 10670−10673.
(30) At the MP2/6-31G(d) level, the relative energies (in kcal/mol) of transition-state structures for enolborane addition to **2** are: **2A** (+2.8), **2B** (0), **2C** (+0.4), **2A′** (+1.7), **2B′** (+0.6), **2C′** (+2.4).

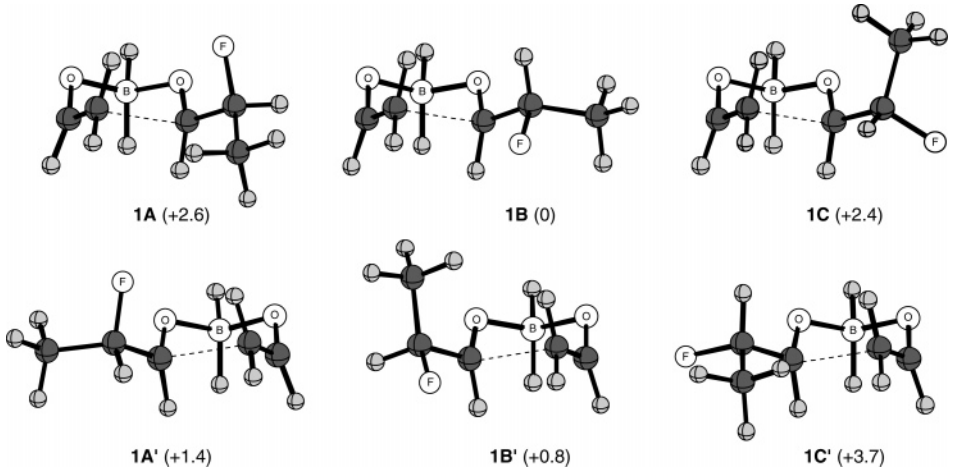

Figure 8. Transition-state structures for enolborane addition to **1** (relative energy in kcal/mol).

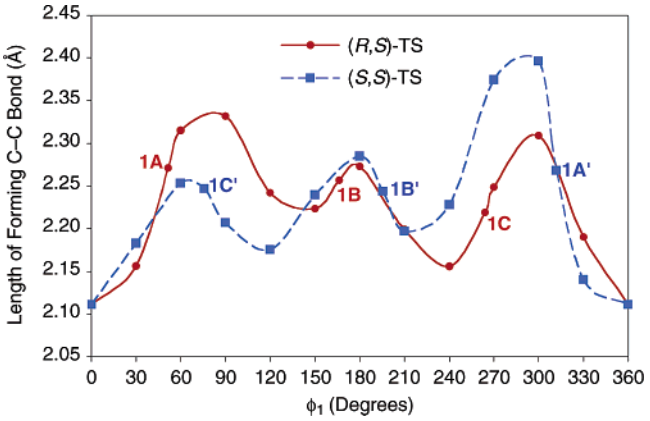

Figure 9. TS C−C bond length for enolborane addition to **1** as a function of dihedral angle ϕ_1.

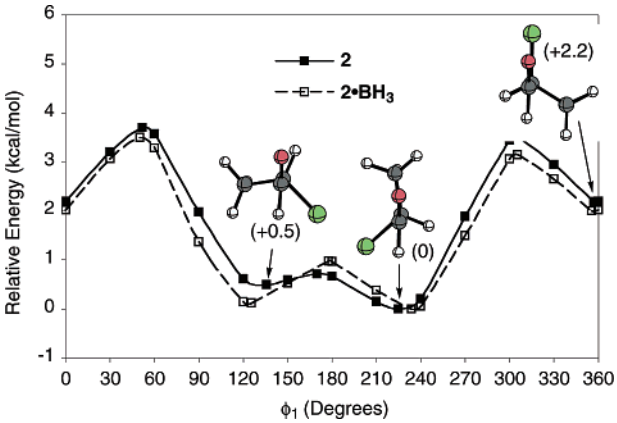

Figure 11. Rotational energy profile of **2** and **2**·BH_3 (red = O, green = Cl).

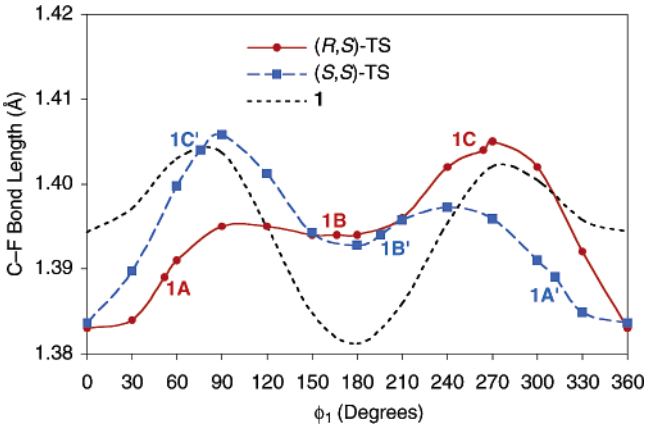

Figure 10. TS C−F bond length for enolborane addition to **1** as a function of dihedral angle ϕ_1.

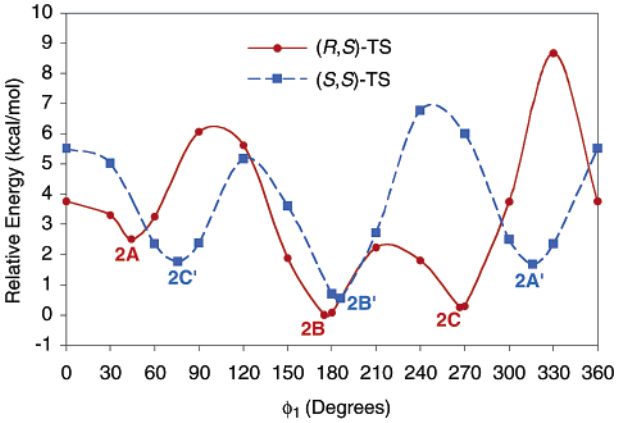

Figure 12. Relative TS energy for enolborane addition to **2** as a function of dihedral angle ϕ_1.

enolborane (Figure 14). In this case, the transition-state structures **2A**,**B** and **2A′**,**B′** are all characterized by a 2.23 Å distance for the forming C−C bond, while structures **2C** and **2C′** contain significantly shorter C−C distances (2.15 and 2.18 Å, respectively). The involvement of the C−Cl bond in the Nu → σ^*_{C-Cl} hyperconjugative interaction believed to stabilize PFA transition states **C** and **C′** can be assessed by analyzing the C−Cl bond lengths in both the transition-state structures and reactant aldehyde structures (Figure 15).[28] Indeed, **2C** and **2C′** are characterized by the longest C−Cl bonds (**2C**, 1.843; **2C′**, 1.842 Å) of any transition-state structure. This trend is also observed in the reactant aldehyde **2** (C−Cl range: 1.804−1.833 Å), but the magnitude of the lengthening is somewhat reduced relative to the transition-state structures **2C** and **2C′**. While this can be attributed to a transition-state Nu → σ^*_{C-Cl} hyperconjugative interaction, it is difficult to determine the energetic stabilization associated with this delocalization. We later show that for most heteroatom substituents studied, transition-state hyperconjugative interactions of this nature are insignificant relative to other effects.

The disparate behavior of fluoropropanal and chloropropanal indicates that a single model may not adequately describe

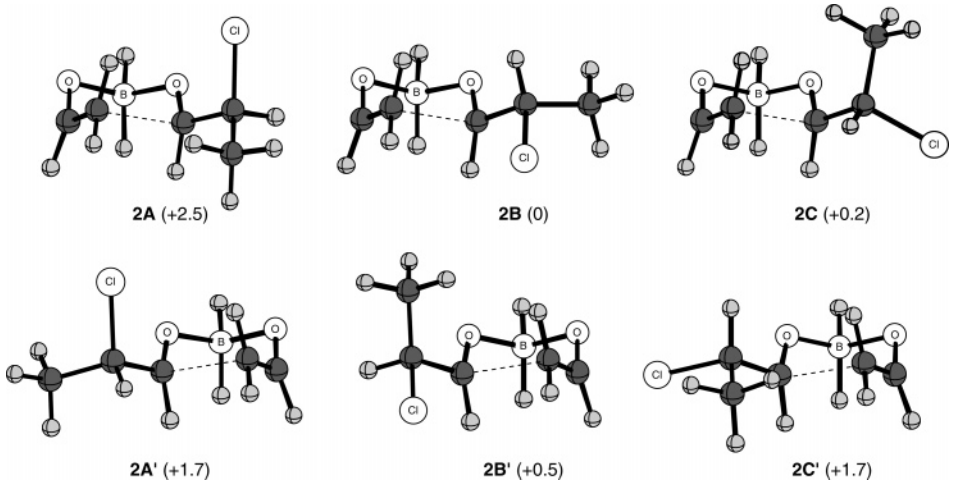

Figure 13. Transition-state structures for enolborane addition to **2** (relative energy in kcal/mol).

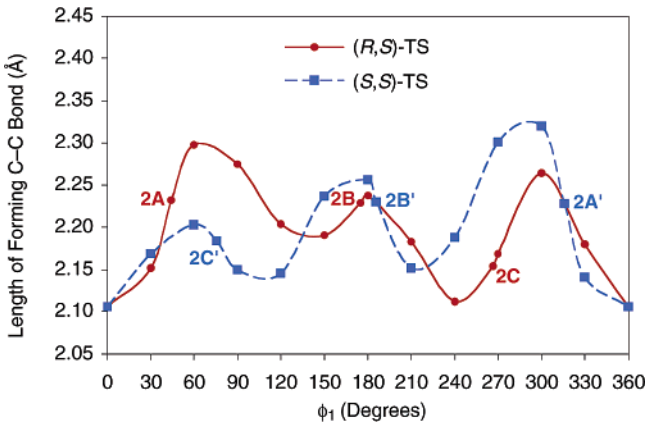

Figure 14. TS C−C bond length for enolborane addition to **2** as a function of dihedral angle ϕ_1.

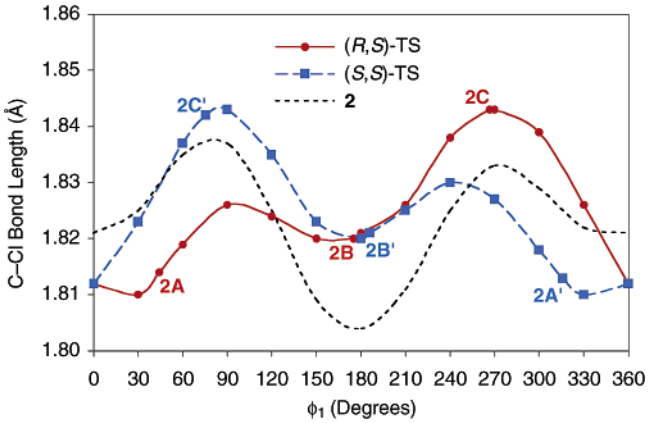

Figure 15. TS C−Cl bond length for enolborane addition to **2** as a function of dihedral angle ϕ_1.

enolborane addition reactions of all heteroatom-substituted aldehydes. It was of interest to determine the relevance of Cornforth and PFA transition-state structures in reactions of propanals **3**−**6** containing group V and VI substituents.[31] Due to the complexity introduced by the additional axis of rotation present in these substituents, only those transition-state structures corresponding to the Cornforth and PFA models for the formation of the anti product diastereomer were considered. While this restriction provides a limited view of the entire potential energy surface of enolborane addition to these aldehydes, it facilitates the study of what are the most relevant structures in terms of current transition-state models.

(31) Aldehydes **3**−**6** contain X−CH_3 fragments, which in some transition-state rotamers could serve as hydrogen bond donors for the aldehyde carbonyl. Analysis of the C−H bond lengths of the X−CH_3 groups, however, provides little evidence for such an interaction. For a recent theoretical investigation of C−H bonds as hydrogen bond donors, see: Alabugin, I. V.; Manoharan, M.; Peabody, S.; Weinhold, F. *J. Am. Chem. Soc.* **2003**, *125*, 5973−5987.

Table 3. Calculated Relative Energies (kcal/mol) for Enolborane Addition to **3** and **4**

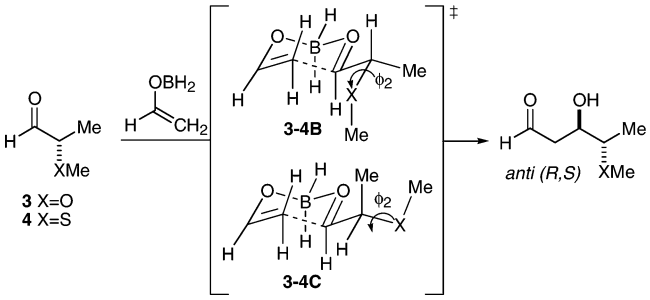

X = O				X = S			
TS	ϕ_1 (deg)	ϕ_2 (deg)	rel E^a	TS	ϕ_1 (deg)	ϕ_2 (deg)	rel E^a
$3B_1$	167.3	77.1	2.5	$4B_1$	177.4	75.5	3.3
$3B_2$	**171.4**	**193.9**	**0**	$4B_2$	173.9	183.8	3.3
$3B_3$	–	–	–	$4B_3$	–	–	–
$3C_1$	266.6	75.2	1.7	**$4C_1$**	**270.8**	**71.0**	**0**
$3C_2$	264.5	206.1	2.4	$4C_2$	274.9	213.6	2.7
$3C_3$	267.2	271.3	2.0	$4C_3$	269.8	278.5	2.0

[a] Relative energy is given in kcal/mol.

Transition-State Structures for 3 and 4. Parameters for the optimized transition-state structures for enolborane addition to 2-methoxypropanal (**3**) and 2-(methylthio)propanal (**4**) are presented in Table 3. In principle, three transition-state structures are expected for a given value of ϕ_1, due to 3-fold rotational isomerism about the C−X bond. It was possible to optimize two Cornforth and three PFA transition-state structures. The missing Cornforth structure denoted $\mathbf{B}_3$ could not be obtained due to a destabilizing *syn*-pentane interaction between the X−CH_3 bond and the forming C−C bond that occurs at $\phi_2 = 300°$. In the case of 2-methoxypropanal, the Cornforth structure $\mathbf{3B}_2$ is lowest in energy, with the nearest PFA structure $\mathbf{3C}_1$ calculated to be 1.7 kcal/mol higher in energy (Figure 16). This situation resembles that found for 2-fluoropropanal. For addition

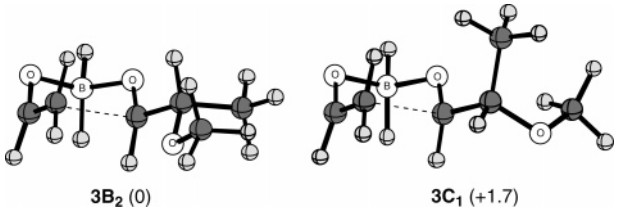

Figure 16. Most stable transition-state structures (of B/C) for enolborane addition to **3** (relative energy in kcal/mol).

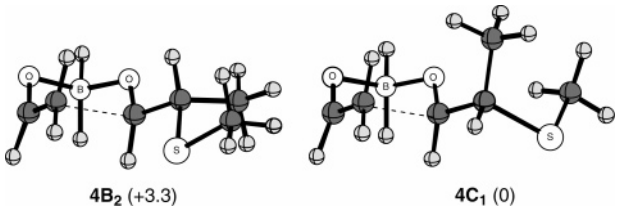

Figure 17. Most stable transition-state structures (of B/C) for enolborane addition to **4** (relative energy in kcal/mol).

Table 4. Calculated Relative Energies (kcal/mol) for Enolborane Addition to **5** and **6**

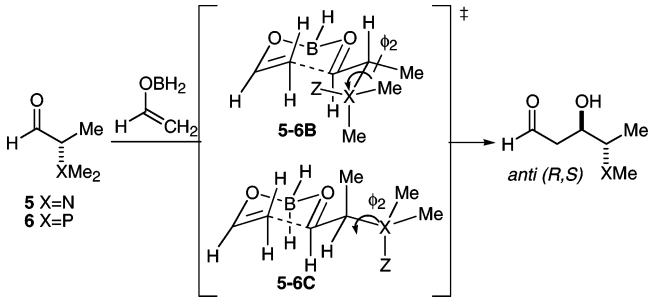

	X = N				X = P		
TS	ϕ_1 (deg)	ϕ_2 (deg)	rel E^a	TS	ϕ_1 (deg)	ϕ_2 (deg)	rel E^a
$5B_1$	–	–	–	$6B_1$	–	–	–
$5B_2$	–	–	–	$6B_2$	–	–	–
$5B_3$	172.3	321.5	0.8	$6B_3$	175.0	318.7	3.5
$5C_1$	260.4	28.7	3.5	$6C_1$	282.9	75.3	1.6
$5C_2$	**272.1**	**174.2**	**0**	**$6C_2$**	**275.5**	**181.7**	**0**
$5C_3$	266.4	323.4	0.1	$6C_3$	272.5	316.5	0.8

[a] Relative energy is given in kcal/mol.

to 2-(methylthio)propanal, however, a dramatic reversal in relative energy is observed. The PFA structure $\mathbf{4C}_1$ is now lowest in energy (Figure 17), with Cornforth structures $\mathbf{4B}_1$ and $\mathbf{4B}_2$ both calculated to be 3.3 kcal/mol higher in energy. Therefore, group VI substituents exhibit markedly different transition-state preferences, with methoxy favoring the Cornforth structure and methylthio favoring the PFA structure.

Transition-State Structures for 5 and 6. Parameters for the optimized transition-state structures for enolborane addition to 2-dimethylaminopropanal (**5**) and 2-dimethylphosphinopropanal (**6**) are presented in Table 4. It was possible to optimize one Cornforth and three PFA transition-state structures. The missing Cornforth structures $\mathbf{B}_2$ and $\mathbf{B}_3$ could not be obtained due to destabilizing *syn*-pentane interactions between the X−CH_3 bond and the forming C−C bond that occur at $\phi_2 = 60$ and 180°. Of the transition-state structures calculated for addition to 2-dimethylaminopropanal, the PFA structure $\mathbf{5C}_2$ (Figure 18) is lowest in energy, with the Cornforth structure $\mathbf{5B}_3$ destabilized by 0.8 kcal/mol. For 2-dimethylphosphinopropanal (Figure 19), the PFA structures are even more favored, with the Cornforth

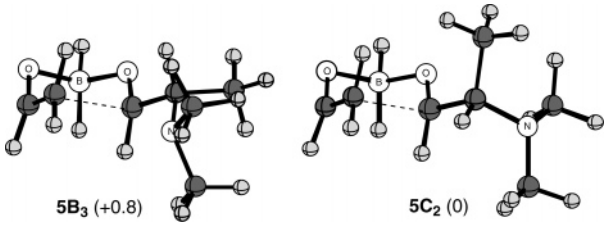

Figure 18. Most stable transition-state structures (of B/C) for enolborane addition to **5** (relative energy in kcal/mol).

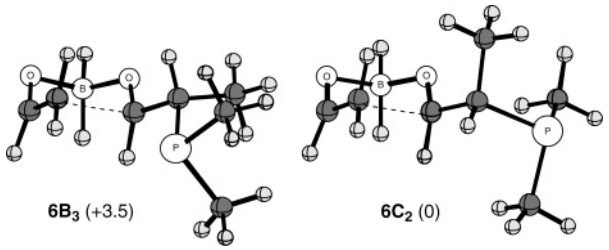

Figure 19. Most stable transition-state structures (of B/C) for enolborane addition to **6** (relative energy in kcal/mol).

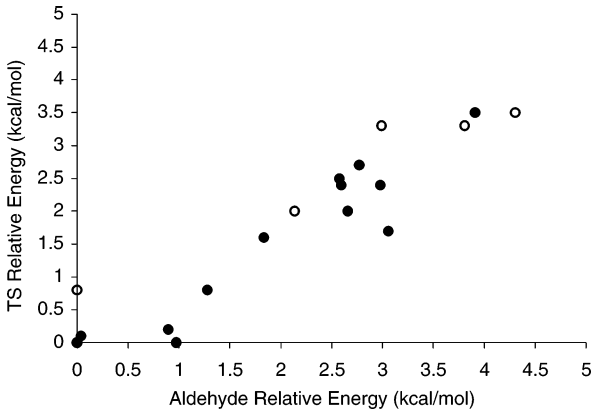

Figure 20. TS energy vs aldehyde energy (of the same ϕ_1 and ϕ_2) for transition structures B and C of **1**−**6**. ○ = TS B, ● = TS C. Five points overlap at 0,0.

structure $\mathbf{6B}_3$ destabilized by 3.5 kcal/mol. Therefore, both first- and second-row group V substituents prefer PFA transition-state structures.

The relative energy of Cornforth or PFA transition-state structures for the formation of the anti product diastereomer in enolborane additon reactions is therefore greatly dependent on the nature of the heteroatom substituent. Chlorine, oxygen, and fluorine substituents are characterized by a preference for the Cornforth arrangement, with the magnitude of the preference increasing in that order. The PFA arrangement is favored by nitrogen, sulfur, and phosphorus substituents, with the magnitude of the preference increasing in that order. These trends could be the result of heteroatom-dependent transition-state interactions, or may simply be the result of conformational preferences intrinsic to the reactant aldehydes. The latter possibility was investigated by determining the relative energy of the reactant aldehydes at fixed dihedral angles ϕ_1 (and ϕ_2 if applicable) corresponding to transition states **B** and **C** of aldehydes **1**−**6**. The roughly linear relationship (Figure 20) between the reactant aldehyde energy and transition-state energy indicates that the transition state for enolborane addition is quite sensitive to the energy of the reactant aldehyde rotamer. Therefore, the proposed transition-state hyperconjugative interaction (Nu → σ^*_{C-X}) that

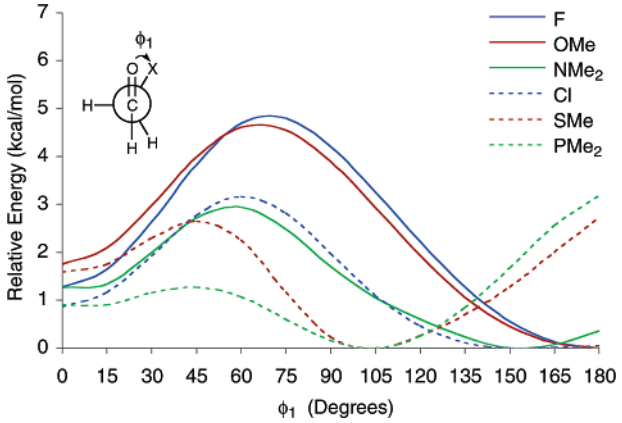

Figure 21. Rotational energy profile for substituted acetaldehydes X−CH_2−CHO. For X = OMe, NMe_2, SMe, and PMe_2, ϕ_2 = 180, 30, 300, and 60°, respectively.

forms the basis of the PFA model appears to be of little significance in determining the relative energy of the transition-state rotamers **B** and **C**.[32]

The ability of α-heteroatom-substituted aldehydes to adopt dihedral angles corresponding to the PFA or Cornforth transition-state structures was investigated for the simplified system of α-substituted acetaldehydes (XCH_2CHO), in which C=O ↔ C−X interactions can be studied without the asymmetry introduced by an α-methyl substituent. The aldehydes were optimized at fixed values of ϕ_1 (0−180° in increments of 15°) and, when applicable, at fixed values of ϕ_2 (0−360° in increments of 30°). The resulting energy profiles for rotation about ϕ_1 are presented in Figure 21. For substituents exhibiting additional rotational isomerism about ϕ_2, the overall lowest energy profile at a single value of ϕ_2 was selected.[33] Comparison of the profiles reveals an interesting parallel between fluorine and oxygen, chlorine and nitrogen, and sulfur and phosphorus with respect to the energy difference between structures with roughly 90 and 180° dihedral angles, which are values of ϕ_1 associated with the PFA and Cornforth transition states. For fluorine and methoxy-substituted acetaldehydes, a large energetic cost is associated with a dihedral angle of 90°. This is significantly less so for acetaldehydes with chlorine or dimethylamino substituents. For methylthio- and dimethylphosphino-substituted acetaldehydes, the situation is reversed, with the nearly perpendicular dihedral angles greatly favored over the antiperiplanar dihedral angles.

The extent to which hyperconjugation between the C=O and C−X bonds stabilizes approximately perpendicular (ϕ_1 = 90°) acetaldehyde rotamers was assessed by natural bond orbital (NBO) analysis[34] of the optimized structures from Figure 21. The NBO delocalization energy (E2) corresponding to the $\pi_{C=O} \rightarrow \sigma^*_{C-X}$ interaction is presented in Figure 22, while that corresponding to the $\sigma_{C-X} \rightarrow \pi^*_{C=O}$ interaction is presented in Figure 23.[35] The delocalization energy of a C−H bond in acetaldehyde is included as a reference. The $\pi_{C=O} \rightarrow \sigma^*_{C-X}$ interaction is present for all C−X bonds and reaches maximum values in the vicinity of ϕ_1 = 90°. The strongest acceptor for $\pi_{C=O}$ is σ^*_{C-F}, while the weakest acceptor is σ^*_{C-P}. The $\sigma_{C-X} \rightarrow \pi^*_{C=O}$ interaction (Figure 23) in which the C−X bond serves as a donor is much greater in magnitude for the second-row heteroatoms. The strongest donor for $\pi^*_{C=O}$ is σ_{C-P}, while the weakest donor is σ_{C-F}.[36] It is interesting to note that the C−H bond of acetaldehyde parallels the C−S bond in donating ability to $\pi^*_{C=O}$.[37] While the final position of the rotational minima is ultimately due to competition between hyperconjugative, dipole−dipole, and steric interactions, the large magnitude of the $\sigma_{C-X} \rightarrow \pi^*_{C=O}$ delocalization for X = SMe and X = PMe_2 contributes significantly to the nearly perpendicular minima calculated for acetaldehydes bearing these substituents.[38,39]

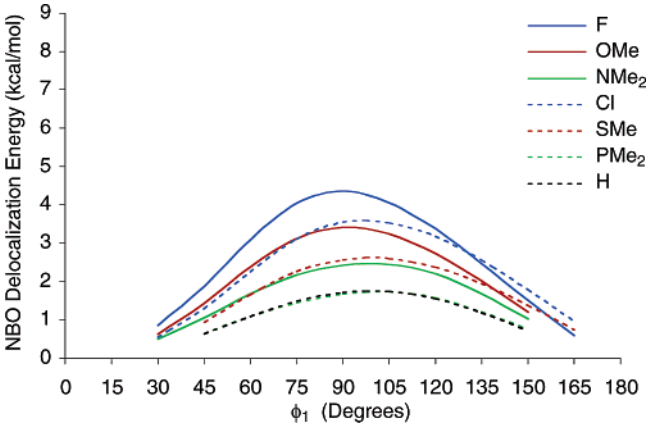

Figure 22. $\pi_{C=O} \rightarrow \sigma^*_{C-X}$ NBO delocalization energy for substituted acetaldehydes X−CH_2−CHO.

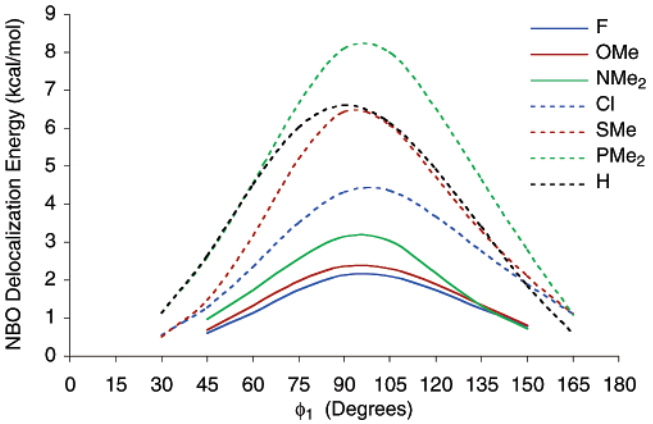

Figure 23. $\sigma_{C-X} \rightarrow \pi^*_{C=O}$ NBO delocalization energy for substituted acetaldehydes X−CH_2−CHO.

Transition-State Structures for Substituted Enolborane Nucleophiles and Aldehyde 3. The aldehyde π-facial selectivity resulting from the reaction of substituted enolborane nucleo-

(32) A recent theoretical study of 5-substituted-2-adamantylidine C−H and O−H insertion reactions has found that the asymmetric induction in this system is due to the conformational energies of the reactant carbenes, rather than to hyperconjugative interactions: Kaneno, D.; Tomoda, S. *Org. Lett.* **2003**, *16*, 2947−2949.

(33) For the complete rotational energy profile as a function of ϕ_1 and ϕ_2 for aldehydes containing divalent and trivalent heteroatom substituents, see the Supporting Information.

(34) Weinhold, F. In *Encyclopedia of Computational Chemistry*; Schleyer, P. v. R., Ed.; Wiley: New York, 1998; pp 1792−1811.

(35) The features of the NBO analysis of 2-methoxypropanal conformers by Cossío and co-workers (ref 25b) are consistent with the analysis of substituted acetaldehyde rotamers presented here.

(36) The relative ability of the C−X bond to serve as a σ donor for $\pi^*_{C=O}$ is approximately the same as that determined for C−X donation to σ^*_{C-H} in substituted ethanes: Alabugin, I. V.; Zeidan, T. A. *J. Am. Chem. Soc.* **2002**, *124*, 3175−3185.

(37) The $\sigma_{C-X} \rightarrow \pi^*_{C=O}$ delocalization energy is significantly greater for X = H in acetaldehyde (6.6 kcal/mol at ϕ_1 = 90°) than for X = CH_3 in propanal (4.4 kcal/mol at ϕ_1 = 90°), indicating that a C−H bond is a better donor for $\pi^*_{C=O}$ than a C−C bond.

(38) The lowest-energy conformation of 2-silylacetaldehyde is calculated to have ϕ_1 = 85.9° (MP2/6-31G(d)//HF/6-31G(d)). This feature has been attributed to $\sigma_{C-Si} \rightarrow \pi^*_{C=O}$ delocalization: Fleming, I.; Hrovat, D. A.; Borden, W. T. *J. Chem. Soc., Perkin Trans. 2* **2001**, 331−338.

Table 5. Calculated Relative Energies (kcal/mol) for *Z*-Enolborane Addition to **3**

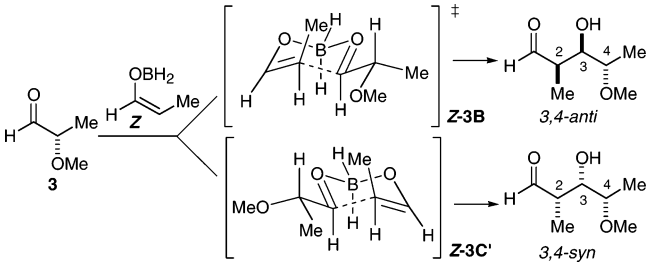

3,4-anti				3,4-syn			
TS	ϕ_1 (deg)	ϕ_2 (deg)	rel E^a	TS	ϕ_1 (deg)	ϕ_2 (deg)	rel E^a
Z-3B$_1$	165.0	75.1	2.3	*Z*-3C′$_1$	54.6	57.1	5.5
Z-3B$_2$	170.2	189.7	0	*Z*-3C′$_2$	–	–	–
Z-3B$_3$	–	–	–	*Z*-3C′$_3$	74.1	277.1	1.2

[a] Relative energy is given in kcal/mol.

Table 6. Calculated Relative Energies (kcal/mol) for *E*-Enolborane Addition to **3**

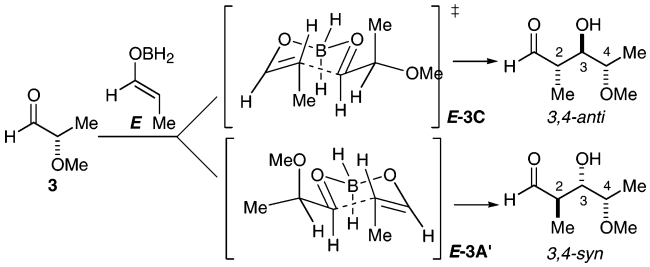

3,4-anti				3,4-syn			
TS	ϕ_1 (deg)	ϕ_2 (deg)	rel E^a	TS	ϕ_1 (deg)	ϕ_2 (deg)	rel E^a
E-3C$_1$	269.1	74.2	1.0	*E*-3A′$_1$	302.7	77.6	0.1
E-3C$_2$	266.4	204.6	0.3	***E*-3A′$_2$**	**306.7**	**191.4**	**0**
E-3C$_3$	269.1	271.5	0.7	*E*-3A′$_3$	–	–	–

[a] Relative energy is given in kcal/mol.

philes with α-alkoxy aldehydes was found to exhibit a significant dependence on enolborane geometry (eqs 2 and 3).[6] This phenomenon is believed to be due to geometry-dependent conformational constraints imposed by the enolate substituent on the rotamer of the α-stereocenter. The observed relationship between enolate geometry and diastereofacial selectivity has been interpreted as supporting the Cornforth model for asymmetric induction. While this conclusion is quite reasonable given the transition-state preferences of acetaldehyde enolborane and 2-methoxypropanal **3** (Table 3), it was of interest to investigate the reaction of the methyl-substituted enolborane **8** with aldehyde **3** to determine if density functional theory could reproduce the experimentally observed relationship between diastereofacial selectivity and enolate geometry.

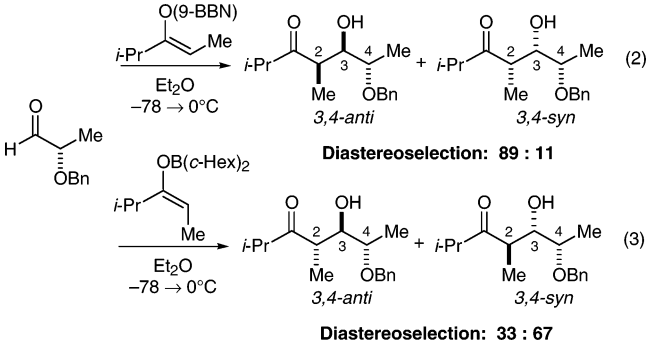

The reaction of 2-methoxypropanal (**3**) with the *E*- and *Z*-enolboranes of propanal (Tables 5 and 6) was chosen as a model of the experimental system (eqs 2 and 3). Due to the proximity of the enolate substituent and α-stereocenter in a cyclic chair transition state, *syn*-pentane interactions that restrict the rotational flexibility of the α-stereocenter are possible. For the reaction of the *Z*-enolborane nucleophile with **3**, the only transition states that avoid *syn*-pentane destabilization are ***Z*-3B** and ***Z*-3C′** (Table 5). Rotational isomerism about the C−O bond of the methoxy substituent results in six possible staggered transition-state structures. It was possible to optimize two transition-state structures corresponding to **B** leading to the anti product diastereomer and two transition-state structures corresponding to **C′** leading to the syn product diastereomer. The Cornforth transition-state structure ***Z*-3B$_2$** is the lowest energy structure by a significant amount. The uncorrected relative energies predict an anti-to-syn ratio of 96:04 at −78 °C, which is in outstanding agreement with the observed ratio of 89:11.

Transition-state structures for the reaction of the *E*-enolborane with aldehyde **3** are presented in Table 6. In this case, rotamers of the aldehyde α-stereocenter corresponding to **C** and **A′** are characterized by the absence of *syn*-pentane interactions with the enolate methyl substituent. Rotational isomerism about the C−O bond of the methoxy substituent results in six possible staggered transition-state structures. Of these, it was possible to optimize three transition-state structures corresponding to the PFA rotamer **C** leading to the anti product diastereomer and two transition-state structures corresponding to the transition-state rotamer **A′** leading to the syn product diastereomer. The PFA structures for the formation of the anti product diastereomer are comparable in energy to the structures leading to the syn product diastereomer. The predicted anti-to-syn ratio derived from the uncorrected relative energies is 24:76 at −78 °C, which is in outstanding agreement with the observed ratio of 33:67. Note that the remarkably good agreement between the predicted and observed diastereomeric ratios may result from some cancellation of errors associated with different borane reagents, differential solvation effects, and differential thermal contributions to activation free energies. Nevertheless, the quality of the agreement suggests that the conformational interpretations discussed above have relevance.

Conclusion

The addition of enolborane nucleophiles to chiral α-heteroatom-substituted aldehydes was investigated using density functional theory by means of B3LYP/6-31G(d) calculations. The relative energy of PFA and Cornforth transition-state structures leading to the anti product diastereomer is found to depend on the nature of the α-heteroatom substituent, with electronegative substituents (F, OMe, Cl) favoring Cornforth structures, while less electronegative substituents (PMe$_2$, SMe, NMe$_2$) favor PFA structures. These preferences are correlated

(39) These findings are reminiscent of Cieplak's premise of transition-state stabilization by interaction of the strongest σ donor with the incipient C−Nu antibond: Cieplak, A. S. *J. Am. Chem. Soc.* **1981**, *103*, 4540−4552. However, since it has already been established (Figure 20) that the transition-state energies are correlated with the aldehyde conformational energies, it is not necessary to invoke such additional transition-state interactions to account for the observed trends.

with the relative energy of the corresponding rotamer of the uncomplexed reactant aldehyde, indicating that the transition states are particularly sensitive to the conformation of the aldehyde. In support of this claim, the calculated rotational energy profiles for α-heteroatom-substituted acetaldehydes reveal significant heteroatom-dependent conformational preferences. These findings indicate that while PFA transition-state structures are important for some heteroatom-substituted aldehydes, the proposed Nu → σ^*_{C-X} interaction which forms the basis of the PFA model is insignificant for enolborane nucleophiles. An accurate model of asymmetric induction in enolborane addition reactions is critically important for predicting the outcome of complex aldol processes. An example is the reaction of substituted enolates and α-alkoxy aldehydes, for which the diastereofacial selectivity exhibits a significant dependence on enolborane geometry. The calculated transition-state structures for the reaction between *Z*- and *E*-enolboranes of propanal with 2-methoxypropanal predict a diastereofacial selectivity that is in good agreement with experiment.

Acknowledgment. Support has been provided by the National Institutes of Health (GM-33328-18) and the National Science Foundation. Fellowship support from the NSF for V.J.C. is also acknowledged. V.J.C. thanks Jesse Kroll (Harvard University) for helpful discussions.

Supporting Information Available: Complete ref 13, Cartesian coordinates of unconstrained reactants and transition-state structures discussed in the text, and conformational energy profiles for acetaldehydes containing divalent and trivalent heteroatom substituents as a function of both ϕ_1 and ϕ_2 are provided. This material is available free of charge via the Internet at http://pubs.acs.org.

JA0555670